CONDUCTING POLYMER/GHASSOUL NANOCOMPOSITES

TOKARSKÝ Jonáš[1,2], KULHÁNKOVÁ Lenka[3], PEIKERTOVÁ Pavlína[1,2], MAMULOVÁ KUTLÁKOVÁ Kateřina[1], PLAČEK Tomáš[3]

[1]VSB - Technical University of Ostrava, Nanotechnology Centre, Ostrava, Czech Republic, EU
[2]VSB - Technical University of Ostrava, IT4Innovations, Ostrava, Czech Republic, EU
[3]VSB - Technical University of Ostrava, Faculty of Metallurgy and Materials Engineering, Ostrava, Czech Republic, EU

Abstract

Ghassoul [rasul], stevensite-rich clay from Morocco, was used as a component of electrically conducting polypyrrole/ghassoul and polyaniline/ghassoul nanocomposites with polymer:clay ratio 1:1. The nanocomposites in powder form were obtained by polymerization of pyrrole and anilinium sulfate, respectively, in aqueous suspension of ghassoul. Ammonium peroxydisulfate was used as an oxidizing agent for the preparation of polyaniline/ghassoul nanocomposite. In case of polypyrrole/ghassoul nanocomposites, two oxidizing agents, ammonium peroxydisulfate and ferric chloride, were tested and compared. Nanocomposites were characterized using X-ray powder diffraction, thermogravimetry, Raman spectroscopy, scanning electron microscopy, and conductivity measurements. Conductivity of nanocomposites in powder form was compared with conductivity of pressed tablets. Tablets pressed from nanocomposite containing polypyrrole synthesized using ferric chloride exhibit significant electrical anisotropy: conductivity in direction parallel to the tablet's plane is ~580× higher than conductivity in direction perpendicular to the tablet's plane. Possible application of tablets as load sensors was tested.

Keywords: Polyaniline, polypyrrole, ghassoul, nanocomposite, conductivity

1. INTRODUCTION

Ellectrically conducting polymers are characterized by π-conjugated structure allowing the conduction of electrical current. Two main representatives - polyaniline (PANI) and polypyrrole (PPy) - attract the attention of scientists for many years and various applications including anti-corrosive coatings, sensors, etc. were developed [1, 2]. Further improvement of electrical properties can be achieved by preparation of nanocomposites combining conducting polymers and layered materials [3, 4]. Natural clay minerals are very suitable for this purpose [5-7].

Ghassoul [rasul] (GHA), clay rich in layered silicate stevensite (smectite group), is mined in the only known deposit in the world, *Jbel Ghassoul* mountain in *Fès-Boulemane region in* Morocco. GHA is studied for a relatively short time (about twenty years) by Moroccan, French, and Spanish materials scientist. It was found to be excellent adsorbent for various organic and metal cations [8, 9] as well as promising precursor for cordierite ceramics [10]. However, almost no attention was paid to GHA as a component of nanocomposites and Nanotechnology Centre in VŠB-TU Ostrava is the first Czech scientific institute where GHA-based functional nanocomposites are prepared and studied.

Present work is focused on preparation and characterization of PPy/GHA and PANI/GHA nanocomposites prepared by polymerization of pyrrole and anilinium sulfate, respectively, in aqueous suspension of GHA. For the preparation of PPy/GHA, two oxidizing agents, $(NH_4)_2S_2O_8$ and $FeCl_3$, were tested and compared. Nanocomposites were characterized using X-ray powder diffraction, thermogravimetry, Raman spectroscopy, scanning electron microscopy, and conductivity measurements.

2. MATERIALS AND METHODS

2.1. Preparation of the samples

All chemicals were used as received from Lach-Ner, Czech Republic. Pure GHA purchased at a local market in Casablanca, Morocco, was dried, milled, and sieved. Size fraction < 40 μm was used. PANI/GHA and PPy_A/GHA samples were prepared from anilinium sulfate and pyrrole, respectively, using $(NH_4)_2S_2O_8$ as oxidizing agent. Amount of GHA added to the reaction mixture was chosen so that the polymer:GHA ratio was 1:1. For PPy_Fe/GHA sample, $FeCl_3$ was used as oxidizing agent. After 6 h stirring of reaction mixtures the obtained solids were collected on filters, rinsed with distilled water (followed by HCl in case of PANI/GHA), and dried at 40 °C for 24 h. Tablets prepared from the powder samples (m = 3 g) were pressed at room temperature without any binder at Zwick 1494 hand press. Applied pressure was 28 MPa.

2.2. Characterization methods

X-ray powder diffraction (XRPD) patterns of all samples pressed in a rotational holder were recorded in reflection mode under $Co_{K\alpha}$ irradiation (λ = 1.7889 Å) using the Bruker D8 Advance diffractometer equipped with a fast position sensitive detector VÅNTEC 1. Phase composition of the samples was evaluated using the ICDD PDF 2 Release 2014 database. STA 409 EP, Netzsch, was used for thermogravimetry (TG) analysis. Samples were heated up to 1100 °C (10 °C·min^{-1}) in dry air with a flow rate 100 cm^3·min^{-1}. Morphology and composition of the samples were studied by scanning electron microscope (SEM) PhilipsXL30 equipped with EDAX analyser. Images were obtained using secondary electron detector. Raman microspectroscopy was performed using Raman microscope XploRA™, Horiba Jobin Yvon, equipped with 532 nm excitation laser source, with 50× objective and using 1200 g/mm grating. Electrical measurements of powders and pressed tablets were performed using devices illustrated schematically in **Figure 1**. Conductivities of tablets were measured in two directions: the in-plane direction ($\sigma_=$) and the direction perpendicular to tablet's plane ($\sigma_\perp$), i.e., the direction of pressure applied during preparation of tablets. Volume of measured powder samples was ~ 60 mm^3 (height of column ~ 5 mm). All measurements were repeated four times and average conductivity values with standard deviations are provided.

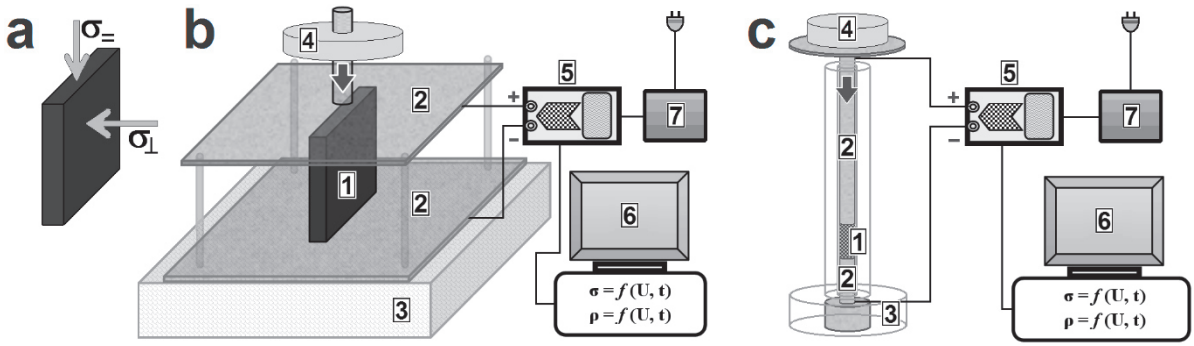

Figure 1 (a) Directions in which the electrical conductivity of tablets was measured. Devices for conductivity measurements of (b) tablets and (c) powders: 1 - sample, 2 - Cu-electrodes, 3 - insulating base, 4 - weight providing constant load, 5 - measuring card PCI-6221, 6 - PC + software, 7 - DC voltage source HY3003D

3. RESULTS AND DISCUSSION

Pure GHA and nanocomposites in powder form were characterized using XRPD (**Figure 2**). GHA contains many phases from which the layered silicate stevensite ($Mg_3Si_4O_{10}(OH)_2$), sepiolite ($Mg_4Si_6O_{15}(OH)_2$), quartz (SiO_2), and celestine ($SrSO_4$) are dominant. Clinoenstatite ($Mg_2Si_2O_6$) and dolomite ($CaMg(CO_3)_2$) as additional phases were found. XRPD patterns of composites exhibit changes in comparison with pure GHA.

Significant shift of basal reflection (d_{001} = 13.97 Å → 17.56 Å) in the case of PPy_Fe/GHA suggests intercalation of PPy. Disappearance of basal reflection in PPy_A/GHA and PANI/GHA spectra is a consequence of presence of sulfates in the preparation mixture causing disordering of the layers.

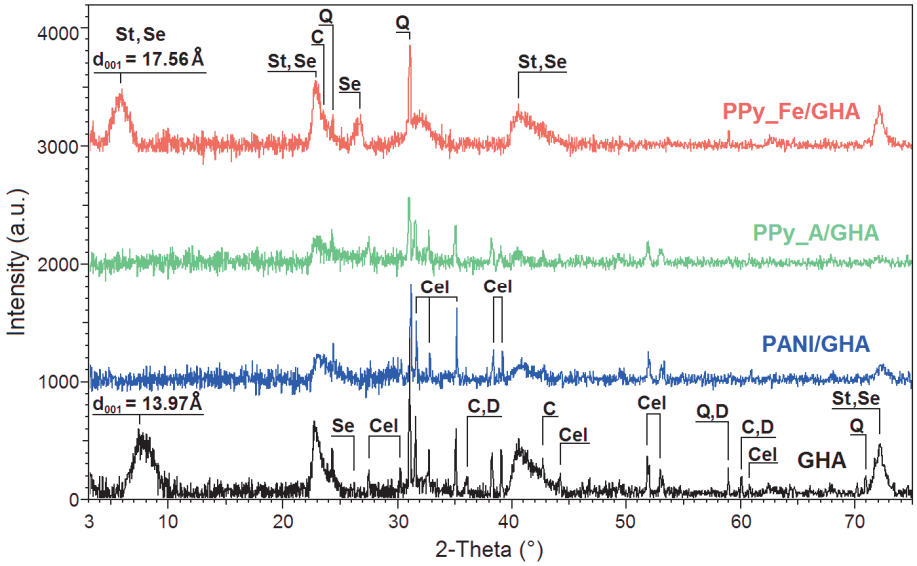

Figure 2 XRPD patterns of pure GHA and prepared composites. C - clinoenstatite, Cel - celestine, D - dolomite, Q - quartz, Se - sepiolite, St - stevensite

TG analysis (**Table 1**) showed higher amount of adsorbed water on the surface of nanocomposites (Δm_1) and negligible difference between GHA and nanocomposites in amount of interlayer water (Δm_2). Loss of organic matter (Δm_3) gives an information about polymer content in composites. Dehydroxylation of clays occurs in the range 750-950 °C (Δm_4) and weight loss above 950 °C (Δm_5) can be attributed to the decomposition of carbonates.

Table 1 Weight losses of GHA and composites revealed by TG analysis

Sample	Δm_1 (%) (30-110°C)	Δm_2 (%) (110-250°C)	Δm_3 (%) (250-750°C)	Δm_4 (%) (750-950°C)	Δm_5 (%) (950-1100°C)
GHA	1.9	3.4	-	2.0	2.8
PPy_A/GHA	5.8	3.1	52.4	-	-
PPy_Fe/GHA	3.8	3.1	48.6	-	-
PANI/GHA	4.0	3.3	40.4	-	-

Due to the fluorescence of pure GHA [11], Raman spectra are shown only for the nanocomposites (**Figure 3**). For PPy-containing samples, the band ~1590 cm^{-1} (C=C backbone stretching) arises from polaron and bipolaron structures [12]. Broad band 1320-1390 cm^{-1} is associated with ring stretching vibrations. C-H and N-H in-plane deformation quinoid polaron vibration is located at 1058 cm^{-1} [12, 13]. While for the PPy_A/GHA sample bands at 977 cm^{-1} (ring deformation - polaron) and 936 cm^{-1} (ring deformation - bipolaron) [13] have the same intensity, in case of PPy_Fe/GHA the band at 936 cm^{-1} is more intensive than band at 977 cm^{-1}. The band at 1254 cm^{-1} (quinoid bipolaron structure) [14,15] is also more intensive in PPy_Fe/GHA spectrum.

Spectrum of PANI/GHA (sample contains all main characteristic PANI bands (**Figure 3**). The most intesive band at 1600 cm^{-1} is associated with C=C vibrations in quinone, while bands at 1529 cm^{-1} and 1630 cm^{-1} arise from vibrations of benzene rings. Other observed bands: 1581 (C=C in quinone), 1420 cm^{-1} (C-C stretching in

quinone and protonated oxazine-like units), 1270 cm^{-1} (C-N vibrations of various benzenoid and quinoid forms, benzene ring deformations), 1186 cm^{-1} (C-H bending), and 828, 532, 426 cm^{-1} (out-of-plane and deformation vibrations of various substituted aromatic rings) [16]. Low intensity of protonation band (C-$N^{+\cdot}$ vibration, related to conductivity [16]) at 1345 cm^{-1} suggests low conductivity of PANI/GHA sample.

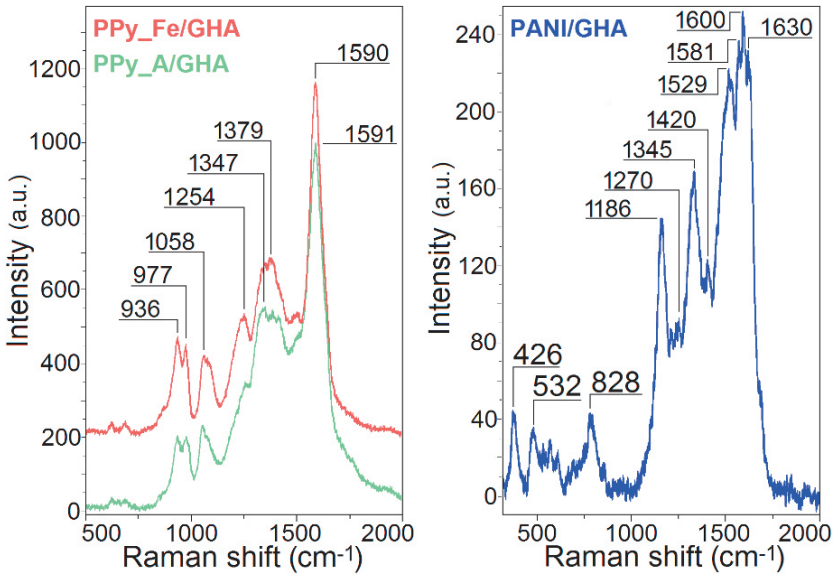

Figure 3 Raman spectra of prepared composites

Morphology of GHA and nanocomposites was studied using SEM analysis (**Figure 4**). Comparison of SEM images showed full coverage of GHA by PANI. In case of PPy_A/GHA and PPy_Fe/GHA samples, uncovered areas can be found. While PANI creates dense layer composed of large grains (~ 5 µm), PPy layers in both PPy_A/GHA and PPy_Fe/GHA nanocomposites are more fluffy and composed from smaller grains. Protruding PPy creates links between particles in PPy-contaning nanocomposites which can be seen especially in SEM image of PPy_A/GHA sample. EDS analyses (**Figure 4**) are in good agreement with XRPD (Mg-rich silicates) and presence of polymers in nanocomposites was confirmed by appearance of carbon and nitrogen.

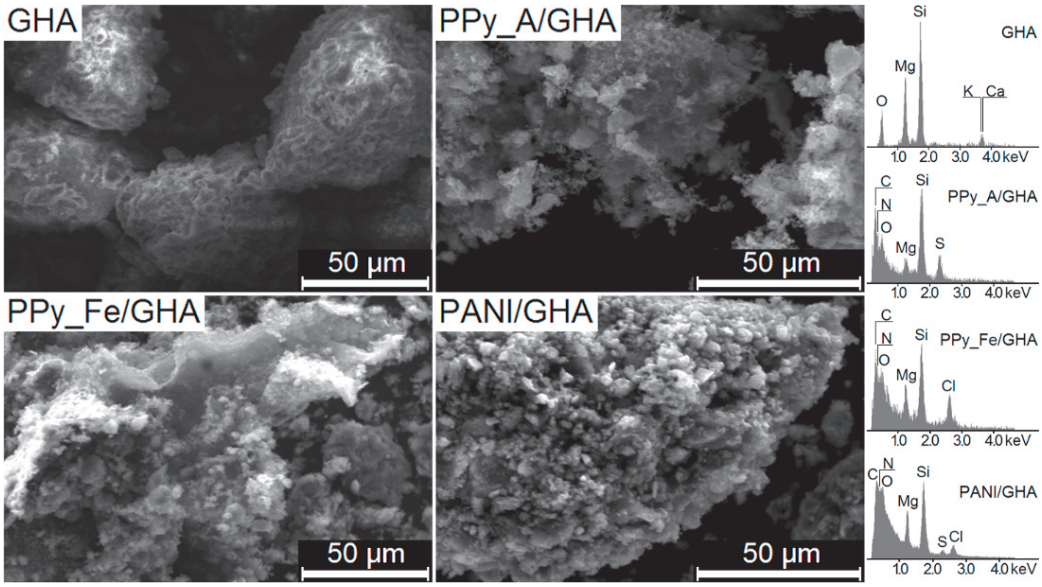

Figure 4 SEM images of GHA and nanocomposites with corresponding results of EDS analysis

Electrical conductivities of samples are summarized in **Table 2**. Measurements of powders and tablets (see measuring devices in **Figure 1**) led to the same trend of conductivity. The difference in σ values comes from different experimental conditions (amount of sample, surface area of electrode, etc.). High σ values of PPy_Fe/GHA are in good agreement with more intensive Raman bands related to bipolarons (**Figure 3**) and correspond well with the successful intercalation process (**Figure 2**). High anisotropy factor ($\sigma_{=} / \sigma_{\perp} = 584$) observed in case of tablet pressed from PPy_Fe/GHA (**Table 2**) can be explained by pressure-induced preferred orientation of platy particles lying parallel to the tablet's plane. Such oriented particles serve as an insulator and reduce the conductivity in the direction perpendicular to the tablet's plane, similarly to previously studied PANI/montmorillonite intercalates [6]. Analogous effect occurs also in case of PPy_A/GHA and PANI/GHA but not so significantly (anisotropy factors are in order of tens). Lower anisotropy can be attributed to disordering of layered structure and disappearance of basal reflections in case of these two samples (**Figure 2**).

Table 2 Electrical conductivities of samples measured in the form of powder and pressed tablets

Sample	Powder	Pressed tablet		
	$\sigma_{\perp}$ (S/m)	$\sigma_{\perp} \cdot 10^3$ (S/m)	$\sigma_{=}$ (S/m)	$\sigma_{=} / \sigma_{\perp}$
PPy_Fe/GHA	33.472 ± 2.341	2.45 ± 0.51	1.430 ± 0.163	584
PPy_A/GHA	0.921 ± 0.104	1.61 ± 0.79	0.125 ± 0.027	78
PANI/GHA	0.742 ± 0.151	0.19 ± 0.11	0.010 ± 0.004	54

Samples in the form of tablets were tested for a potential use as a load sensors. Current responses to increasing and decreasing pressure are shown in **Figure 5**. PPy_A/GHA and PPy_Fe/GHA samples exhibit unequal response to identical pressure during loading and unloading part of the experiment. More stable responses were found for PANI/GHA sample, which is, therefore, promising candidate for further testing.

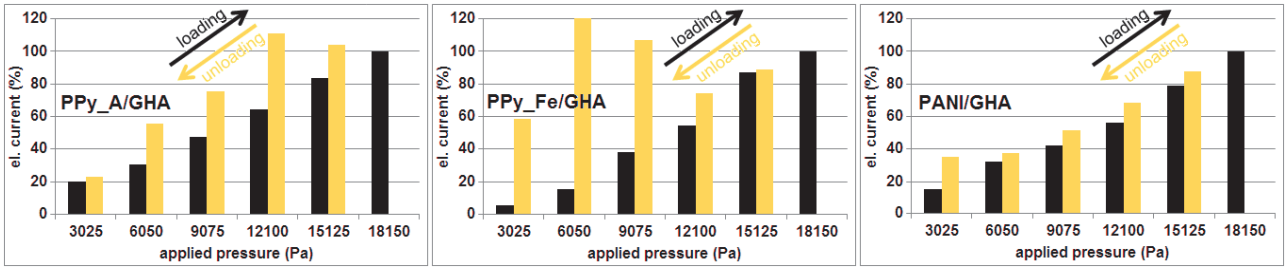

Figure 5 Current responses to external pressure applied on tablets pressed from prepared nanocomposites

4. CONCLUSION

It was demonstrated that stevensite-rich clay GHA can be used for the preparation of conductive polymer-based nanocomposites. However, poor conductivity and anisotropy of PPy_A/GHA and PANI/GHA samples together with disappearance of basal reflection suggest unsuitability of the ammonium peroxydisulfate as an oxidizing agent. In order to obtain high conductivity, pyrrole oxidized by ferric chloride is much more suitable as proven by conductivity measurements performed on PPy_Fe/GHA sample. Use of ferric chloride led also to the succesful intercalation and also high anisotropy in conductivity was observed for PPy_Fe/GHA sample. On the other hand, the current response to external pressure is quite stable only for the low conductive PANI/GHA sample, as revealed during experiment testing the possible use of tablets pressed from the nanocomposites as load sensors. More conductive PPy_A/GHA and PPy_Fe/GHA nanocomposites do not seem to be suitable for this purpose.

ACKNOWLEDGEMENTS

This research has been funded by the NPU II - IT4Innovations excellence in science (project no. LQ1602) and the Ministry of Education, Youth and Sports of the Czech Republic (project no. SP2016/63). Authors thank S. Vallová for TG measurements.

REFERENCES

[1] PERRIN F. X., PHAN, T. A., NGUYEN D. L. Preparation and characterization of polyaniline in reversed micelles of decylphosphonic acid for active corrosion protection coatings. *European Polymer Journal*, 2015, vol. 66, pp. 253-265.

[2] KOIRALA, K., Sevilla III, F. F., Santos, J. H. Biomimetic potentiometric sensor for chlorogenic acid based on electrosynthesized polypyrrole. *Sensors and Actuators B: Chemical*, 2016, vol. 222, pp. 391-396.

[3] KHAN, A., KHAN, A. A. P., RAHMAN, M. M., ASIRI, A. M. High performance polyaniline/vanadyl phosphate (PANI-VOPO4) nano composite sheets prepared by exfoliation/intercalation method for sensing applications. *European Polymer Journal*, 2016, vol. 75, pp. 388-398.

[4] WANG, J., WU, Z., HU, K., CHEN, X., YIN, H. High conductivity graphene-like MoS_2/polyaniline nanocomposites and its application in supercapacitor. *Journal of Alloys and Compounds*, 2015, vol. 619, pp. 38-43.

[5] PIROMRUEN, P., KONGPARAKUL, S., PRASASSARAKICH, P. Synthesis of polyaniline/montmorillonite nanocomposites with an enhanced anticorrosive performance. *Progress in Organic Coatings*, 2014, vol. 77, no. 3, pp. 691-700.

[6] TOKARSKÝ, J., MAMULOVÁ KUTLÁKOVÁ, K., NEUWIRTHOVÁ, L., KULHÁNKOVÁ, L., STÝSKALA, V., MATĚJKA, V., ČAPKOVÁ, P. Texture and electrical conductivity of pellets pressed from PANI and PANI/montmorillonite intercalate. *Acta Geodynamica et Geomaterialia*, 2013, vol. 10, no. 3, pp. 371-377.

[7] RAMÔA, S. D. A. S., BARRA, G. M. O., MERLINI, C., SCHREINER, W. H., LIVI, S., SOARES, B. G. Production of montmorillonite/polypyrrole nanocomposites through in situ oxidative polymerization of pyrrole: Effect of anionic and cationic surfactants on structure and properties. *Applied Clay Science*, 2015, vol. 104, pp. 160-167.

[8] BENHAMMOU, A., YAACOUBI, A., NIBOU, L., TANOUTI, B. Adsorption of metal ions onto Moroccan stevensite: kinetic and isotherm studies. *Journal of Colloid and Interface Science*, 2005, vol. 282, no. 2, pp. 320-326.

[9] ELASS, K., LAACHACH, A., ALAOUI, A., AZZI, M. Removal of methylene blue from aqueous solution using ghassoul, a low-cost absorbent. *Applied Ecology and Environmental Research*, 2010, vol. 8, no. 2, pp. 153-163.

[10] BEJJAOUI, R., BENHAMMOU, A., NIBOU, L., TANOUTI, B., BONNET, J. P., YAACOUBI, A., AMMAR, A. Synthesis and characterization of cordierite ceramic from Moroccan stevensite and andalusite. *Applied Clay Science*, 2010, vol. 49, no. 3, pp. 336-340.

[11] FROST, L. R., RINTOUL, L. Lattice vibrations of montmorillonite: an FT Raman and X-ray diffraction study. *Applied Clay Science*, 1996, vol. 11, no. 2-4, pp. 171-183.

[12] GUPTA, S. Hydrogen bubble-assisted syntheses of polypyrrole micro/nanostructures using electrochemistry: structural and physical property characterization. *Journal of Raman Spectroscopy*, 2008, vol. 39, no. 10, pp. 1343-1355.

[13] OMASTOVÁ, M., MASNÁČKOVÁ, K., FEDORKO, P., TRCHOVÁ, M., STEJSKAL, J. Polypyrrole/silver composites prepared by single-step synthesis. *Synthetic Metals*, 2013, vol. 166, no. 10, pp. 57-62.

[14] TABAČIAROVÁ, J., MIČUŠÍK, M., FEDORKO, P., OMASTOVÁ, M. Study of polypyrrole aging by XPS, FTIR and conductivity measurements. *Polymer Degradation and Stability*, 2015, vol. 120, pp. 392-401.

[15] SU, N., LI, H. B., YUAN, S. J., YI, S. P., YIN, E. Q. Synthesis and characterization of polypyrrole doped with anionic spherical polyelectrolyte brushes. *eXPRESS Polymer Letters*, 2012, vol. 6, no. 9, pp. 697-705.

[16] ŠEDĚNKOVÁ, I., TRCHOVÁ, M., STEJSKAL, J. Thermal degradation of polyaniline films prepared in solutions of strong and weak acids and in water - FTIR and Raman spectroscopic studies. *Polymer Degradation and Stability*, 2008, vol. 93, no. 12, pp. 2147-2157.